Edinburgh Research Explorer

The Importance of Being Exchanged: [(Gd4M8II)-M-III(OH)(8)(L)(8)(O2CR)(8)](4+) Clusters for Magnetic Refrigeration

Published In:
Angewandte Chemie International Edition

The Importance of Being Exchanged:
[Gd$^{III}_4$M$^{II}_8$(OH)$_8$(L)$_8$(O$_2$CR)$_8$]$^{4+}$ Clusters for Magnetic Refrigeration**

Thomas N. Hooper,[1] Jürgen Schnack,[2] Stergios Piligkos,[3,*] Marco Evangelisti,[4,*] and Euan K. Brechin[1,*]

[1]EaStCHEM, School of Chemistry, University of Edinburgh, West Mains Road, Edinburgh, EH9 3JJ, UK.

[2]Universität Bielefeld, Fakultät für Physik, Postfach 100131, 33501 Bielefeld, Germany.

[3]Department of Chemistry, University of Copenhagen, Universitetsparken 5, 2100 Copenhagen, Denmark.

[4]Instituto de Ciencia de Materiales de Aragón, CSIC-Universidad de Zaragoza, Departamento de Física de la Materia Condensada, 50009 Zaragoza, Spain.
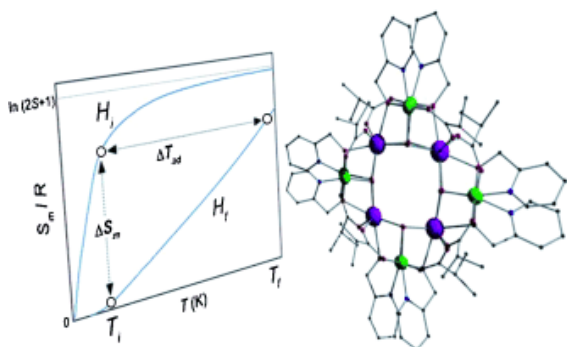
[*]Corresponding authors; S.P.: piligkos@kiku.dk; M.E.: evange@unizar.es; E.K.B.: e.brechin@ed.ac.uk

Graphical abstract:

Abstract

Almost all the constituent parts of the complex $[Ln^{III}_4M^{II}_8(OH)_8(L)_8(O_2CR)_8](X)_4$ – the lanthanide ions (Ln^{3+}), the transition metal ions (M^{2+}), the bridging ligand L, the carboxylates and the counter anions (X) - can be exchanged, allowing for a thorough understanding of the individual contributions to the magneto-caloric effect (MCE).

Main text

One of the most promising applications for molecules built from paramagnetic metal ions is low temperature magnetic refrigeration.[1] Indeed recent studies have suggested that molecular coolers can outperform any conventionally-employed solid-state refrigerant material by orders of magnitude.[2] In order to do so, molecules must possess a combination of a large spin ground state (S), with negligible anisotropy ($D_{cluster} = 0$), weak magnetic exchange between the constituent metal ions and a relatively large metal:non-metal mass ratio (*i.e.* a large magnetic density).[1b] These molecular pre-requisites suggest the use of lanthanide ions and, in particular, the f^7 ion Gd^{3+} in the construction of homo- and heterometallic (Gd-3d) clusters, and a sensible starting point is the synthesis of Gd^{III}-Cu^{II} clusters since previous studies have shown this combination favours ferromagnetic exchange.[3]

Here we introduce a rather remarkable new family of compounds of general formula $[Ln^{III}_4M^{II}_8(OH)_8(L)_8(O_2CR)_8](X)_4$ in which *almost* all the constituent parts – the lanthanide ions (Ln^{3+}), the transition metal ions (M^{2+}), the bridging ligand L, the carboxylates and the counter anions (X) - can be exchanged. In each case the structure remains essentially the same and this allows for a thorough understanding of the individual contributions to the magneto-caloric effect (MCE). In this communication we describe the three family members $[Gd^{III}_4M^{II}_8(OH)_8(L)_8(O_2CR)_8](ClO_4)_4$ (M = Zn, R = CHMe$_2$, **1**; M = Cu, R = CHMe$_2$, **2**; M = Ni, R = CH$_2$Me, **3**; LH = 2-(hydroxymethyl)pyridine) and show how the identity of the transition metal and the *sign* of the magnetic exchange are vital components to consider when designing molecular coolers.

For the sake of brevity we provide a generic structure description, highlighting any differences.   The core (Figure 1 shows complex **2**) of the molecule consists of a square (or wheel) of four corner-sharing $\{Gd^{III}_2M^{II}_2O_4\}^{6+}$ cubanes. The shared corners are the Gd ions which thus themselves form an inner $\{Gd^{III}_4\}$ square, each edge of which is occupied by two μ_3-OH$^-$ ions which further bridge to a M^{II} ion. The μ_3-L$^-$ ions chelate the M^{2+} ions and use their O-arm to further bridge to the second M^{2+} ion in the same cubane and to one Gd ion. There are two carboxylates per cubane, each μ-bridging across a M^{2+}…Gd square face, alternately above and below the plane of the $\{Gd^{III}_4\}$ square.
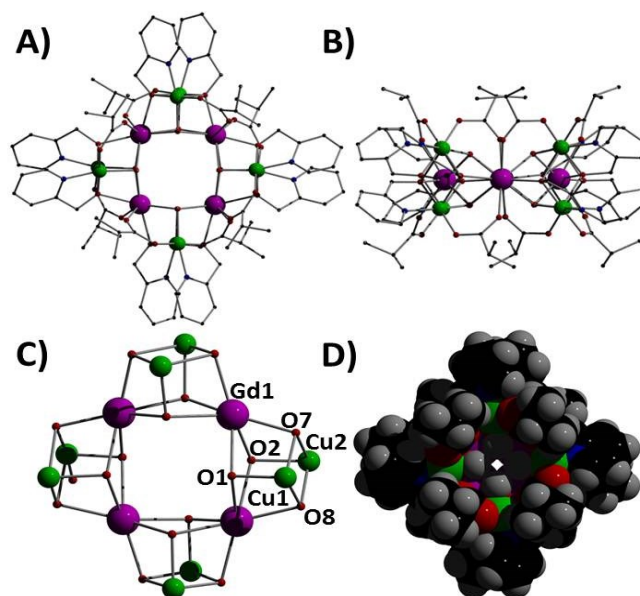
Figure 1. The molecular structure of the cation of complex **2** viewed perpendicular (A) and parallel (B) to the {Gd$_4$} plane. Colour code: Gd^{3+} = purple, Cu^{2+} = green, O = red, N = blue, C = black. H-atoms and the ClO$_4^-$ anions are omitted for clarity. C) The metal-oxygen core, highlighting the corner-sharing {Gd$_2$Cu$_2$O$_4$} cubanes; Cu-O-Cu = 95.64-96.56°; Cu-O-Gd = 95.26-101.87°; Gd-O-Gd = 110.90-111.88°. D) Space filling representation of the cation of **2**.

A comparison of the structure of **1** (Figure S1) with **2** shows them to be very similar. The central {Gd$_4$(OH)$_8$} square motif is almost identical, with the copper structure forming a perfect square (as enforced by crystallographic symmetry) whilst the zinc structure deviates only very slightly, with Gd-Gd-Gd angles of 90.87 and 89.17°. In **2** the Cu^{II} ions are in a square-based pyramidal geometry with the Jahn-Teller axes being the apex of the pyramid. In **1** the L$^-$ ligands have rotated ~45° out of the plane of the face of the cube, affording a more trigonal bipyramidal geometry at the Zn centre, reflecting the lack of electronic stabilisation afforded to a d^{10} ion. Comparison of **1** and **2** with **3** (Figure S2) however does show some significant differences. The bond lengths and angles within the cubes of the {Gd$_4$Ni$_8$} and {Gd$_4$Zn$_8$} structures are similar but the {Gd$_4$(OH)$_8$} motif in **3** has distorted to a more rhombus-like shape, with Gd-Gd-Gd angles of 95.66 and 84.34°. Each Ni^{II} centre is octahedral with six methanol molecules bonding to one nickel centre each, with a change in the coordination of the carboxylates filling the coordination spheres of the remaining two nickel centres. The carboxylate ligands have lost the regular alternating pattern seen in **1** and **2**: six remain in *syn, syn*, μ-coordination mode, bridging across a Gd…Ni square face, but two are now μ$_3$-bridging (Ni…Gd…Ni) in a *syn, syn-anti* fashion across two Gd…Ni square faces.

A search of the CCDC database reveals that there are only two other [Ln$^{III}_4$M$^{II}_8$] complexes reported in the literature, [Gd$^{III}_4$Co$^{II}_8$(OH)$_4$(NO$_3$)$_4$(O$_3$P^{t}Bu)$_8$(O$_2$C^{t}Bu)$_{16}$] and [Gd$^{III}_4$Co$^{II}_8$(O$_3$P^{t}Bu)$_6$(O$_2$C^{t}Bu)$_{16}$].[4] Other molecules with closely related structures are the complex [Dy$^{III}_3$Cu$^{II}_6$L$_6$(OH)$_6$(H$_2$O)$_{10}$]Cl$_2$·ClO$_4$ (LH$_2$ = 1,1,1-trifluoro-7-hydroxy-4-methyl-5-azahept-3-en-2-one) whose structure describes a triangle (or wheel) of three {Dy$^{III}_2$Cu$^{II}_2$O$_4$} cubanes,[5] and the square-in-a-square complexes [Mn$^{III}_4$Ln$^{III}_4$(OH)$_4$(C[4])$_4$(NO$_3$)$_2$(H$_2$O)$_6$](OH)$_2$ (C[4] = calix[4]arene) and [Mn$^{III}_4$Ln$^{III}_4$(μ$_3$-OH)$_4$(N$_3$)$_4$(O$_2$CBu^t)$_8$(t-bdea)$_4$] (t-bdea = t-butyldiethanolamine) containing four corner-sharing {Ln$^{III}_2$Mn^{III}O$_4$] partial cubanes.[6]

The dc magnetic susceptibilities of **1-3** were measured in an applied field, B_0, of 0.1 T over the 5 to 275 K temperature range, and are shown in Figure 2 in the form of $\chi_M T$ products. At 275 K, the obtained $\chi_M T$ values of 31.5, 34.5 and 39.5 cm^3 K mol^{-1} are exactly those expected for spin-only contributions to the magnetism of [Gd$^{III}_4$M$^{II}_8$] (M = Zn, Cu and Ni, respectively) with $g = 2.00$. The temperature dependence of the $\chi_M T$ product of **1** indicates the absence of sizeable exchange interactions between the Gd^{III} ions. The spin-Hamiltonian matrix of **1** is a square matrix of dimension 4096 and can be diagonalised by standard full matrix approaches. The $\chi_M T$ data of **1** can be fitted to a simple isotropic model, containing a unique magnetic exchange-interaction parameter, describing a {Gd$^{III}_4$} square to afford $J_{Gd\text{-}Gd} = 0.02$ cm^{-1}. The temperature dependence of the $\chi_M T$ products of **2** and **3** suggest the presence of ferri- and ferromagnetic exchange interactions, respectively. The data can be successfully fitted with the isotropic model of equation (1), that contains three distinct magnetic exchange-interaction parameters, where $\hat{S}$ is a single-ion spin operator, the index i runs through all twelve centres of **2** and **3** (Gd^{III} ions correspond to indices 1 to 4), $g = 2$ is the isotropic g-factor and μ_B is the Bohr magneton. The spin-Hamiltonian matrix of **2** is of dimension 1,048,576 and cannot be diagonalised in the same way as for **1**. For **2** we used home written software (ITO-MAGFIT[7]) that makes use of Irreducible Tensor Operator algebra[8] to block-diagonalise the spin-Hamiltonian. ITO-MAGFIT is a magnetisation fitting program using the Levenberg–Marquardt algorithm.[9] The best fit exchange parameters determined in this way for **2** are: $J_{CuCu} = 11.84$ cm^{-1}, $J_{GdCu} = -1.38$ cm^{-1} and $J_{GdGd} = 0.20$ cm^{-1}.

$$\hat{H} = g\mu_B B_0 \cdot \sum_i \hat{S}_i +$$
$$\sum \left\{ J_{GdGd}(\hat{S}_1 \cdot \hat{S}_2 + \hat{S}_2 \cdot \hat{S}_3 + \hat{S}_3 \cdot \hat{S}_4 + \hat{S}_4 \cdot \hat{S}_1) \right\} +$$
$$\sum \left\{ J_{MM}(\hat{S}_5 \cdot \hat{S}_6 + \hat{S}_7 \cdot \hat{S}_8 + \hat{S}_9 \cdot \hat{S}_{10} + \hat{S}_{11} \cdot \hat{S}_{12}) \right\} + \qquad (1)$$
$$\sum \left\{ J_{GdM} \begin{bmatrix} \hat{S}_1 \cdot (\hat{S}_5 + \hat{S}_6 + \hat{S}_{11} + \hat{S}_{12}) + \hat{S}_2 \cdot (\hat{S}_5 + \hat{S}_6 + \hat{S}_7 + \hat{S}_8) + \\ \hat{S}_3 \cdot (\hat{S}_7 + \hat{S}_8 + \hat{S}_9 + \hat{S}_{10}) + \hat{S}_4 \cdot (\hat{S}_9 + \hat{S}_{10} + \hat{S}_{11} + \hat{S}_{12}) \end{bmatrix} \right\}$$
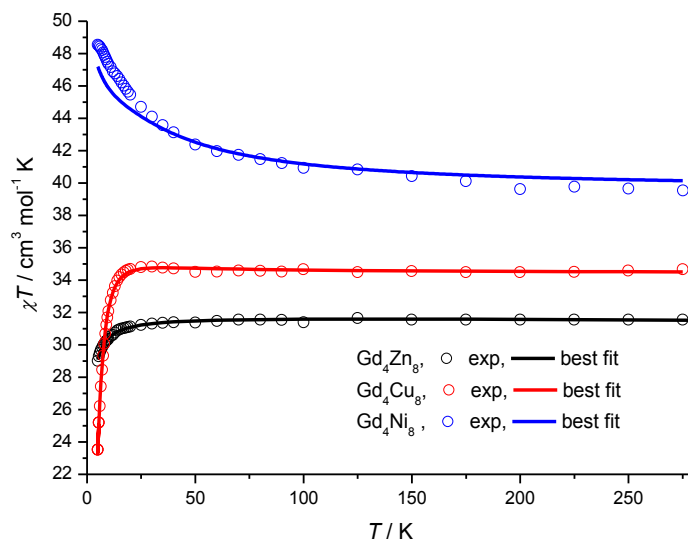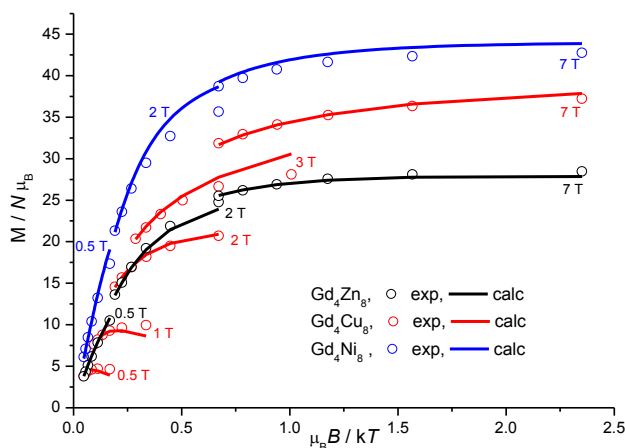
Figure 2. $\chi_M T$ products of **1**, **2** and **3** in a magnetic field of 0.1 T in the temperature range 5 to 275 K. The experimental data have been interpreted as explained in the text.

The spin-Hamiltonian matrix of **3** is of dimension 26,873,856 and cannot be treated by complete matrix diagonalisation. Magnetic observables of such spin systems can nevertheless be accurately determined with the Finite Temperature Lanczos Method.[10] However, since the numerical effort is still enormous the program makes use of open MP parallelisation[11] and has been executed on 40 cores of the SuperMUC Supercomputer at LRZ Garching/Germany as well as on a supercomputer at Bielefeld University.

Thus, the magnetism data of **3** have been interpreted by successive simulations and not by a numerical fitting routine as for **1** and **2**. The obtained exchange parameters are: J_{NiNi} = -24.0 cm^{-1}, J_{GdNi} = -0.34 cm^{-1} and J_{GdGd} = 0.20 cm^{-1}. The $\chi_M T$ product of **3** is very sensitive to the magnitude of the J_{NiNi} exchange interaction. In fact the experimental data could also be reproduced by a parameter set involving an antiferromagnetic Ni-Ni exchange interaction: J_{NiNi} = 6.0 cm^{-1}, J_{GdNi} = -1.32 cm^{-1} and J_{GdGd} = 0.20 cm^{-1}. This uncertainty could not be resolved since simplifying assumptions, such as g = 2.00, had to be made in order to make the numerical treatment feasible at all. Nevertheless, since the Ni-O-Ni angle is approximately 96° the exchange is most likely of ferromagnetic nature - as found in all other Ni^{2+} compounds.[12]

Magnetisation measurements (Figure 3) show saturation values of approximately 28, 38 and 44 $N\mu_B$ for **1-3**, respectively, suggestive of S = 22 for **3**, and field-induced S = 14 and S = 18 ground states for **1** and **2**. The reduced magnetisation data can be reproduced by single point calculations using the parameters determined from the interpretation of the $\chi_M T$ products of **1-3** (Figure 3).

Figure 3. Reduced magnetisation data of **1**, **2**, and **3** in the temperature range 2 to 7 K and the field range 0.5 to 7 T. The experimental data have been interpreted as explained in the text.

The experimental heat capacity (C), normalised to the gas constant R, of the investigated complexes is shown in the left panels of Figure 4, as a function of temperature for selected applied magnetic fields (B_0). As expected, the high-temperature C is dominated by nonmagnetic contributions arising from thermal vibrations of the lattice. At low temperatures, C is dominated by an applied-field sensitive contribution, which shifts to higher temperatures by increasing B_0. No phase transition is detected down to about 0.3 K, indicating that the involved magnetic interactions are weak. From the experimental heat capacity, the temperature dependence of the entropy is obtained by integrating $\int C/T \mathrm{d}T$, leading to the entropy curves depicted in the insets of Figure 4 for the corresponding applied fields. In agreement with the magnetisation data, Fig. 4 shows that the magnetic contributions to the heat capacity extend towards much higher temperatures in the cases of **2** and **3**, proving the presence of (relatively) stronger exchange coupling for these two complexes.

(turn to next page →)
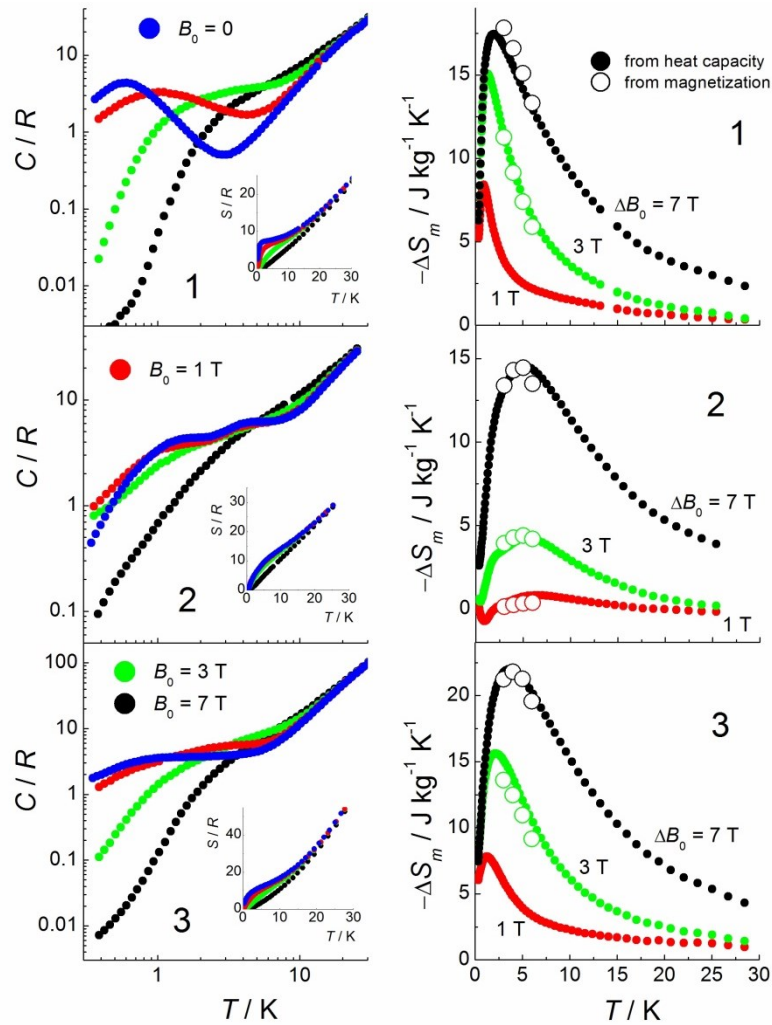
Figure 4. Left: From top to bottom, temperature dependencies of the heat capacities and entropies (insets) of **1**, **2** and **3**, respectively, for selected applied magnetic fields, as labeled. Right: From top to bottom, temperature dependencies of the magnetic entropy changes, as obtained from C (filled dots) and M data (empty dots), for **1**, **2** and **3**, respectively, for selected applied magnetic field changes, as labeled.

Indeed for **1**, the magnetic contribution to the zero-field C takes place at extremely low temperatures, giving rise to an entropy that increases sharply reaching an approximate value of $7R$. The $2\,K < T < 6\,K$ temperature range is characterised by a slow increase of the zero-field entropy, passing from $7.2R$ to $8R$, respectively. Above roughly 6 K, the zero-field entropy starts to steadily increase because of the lattice contribution. The $7 - 8\,R$ plateau can be understood by assuming that all the $Gd^{3+} \cdots Gd^{3+}$ interactions are gradually decoupling. Therefore, we expect the entropy to approach the maximum value for non-interacting single-ion spins, *i.e.* $4 \cdot R \ln(2S_{Gd}+1) = 8.3R$, where $S_{Gd} = 7/2$, in excellent agreement with the experimental data.

The evaluation of the MCE includes the calculation of the magnetic entropy change (ΔS_m) for selected applied field changes (ΔB_0), from the measured heat capacity and magnetisation. As for the former, we can obtain ΔS_m from the temperature and field dependencies of the entropy. The results are summarised in the right panels of Figure 4, together with the estimates obtained by applying the Maxwell relation, $\Delta S_m(T) = \int [\partial M /\partial T] dB_0$ to the magnetisation M data of Fig. 3. We note the nice agreement between the two procedures. For $\Delta B_0 = 7$ T, we observe the largest $-\Delta S_m$ for **3**, since it reaches 22.0 J kg^{-1} K^{-1} at $T =$ 3.6 K. This maximum decreases down to 18.0 J kg^{-1} K^{-1} at $T = 2.0$ K for **1**, close to the full available entropy content of 20.8 J kg^{-1} K^{-1}. For **2**, the maximum $-\Delta S_m$ decreases further, reaching 14.6 J kg^{-1} K^{-1}, although at the relatively higher $T = 5.6$ K. The fact that the Gd-Cu complex has a lower MCE with respect to the Gd-only analogue may seem surprising. The ferrimagnetism of **2** results from the antiferromagnetic $Cu^{2+} \cdots Cu^{2+}$ exchange, and it is thus clear that this type of interaction is the least favourable for observing a large MCE. One can notice that fields higher than ~ 1-2 T are needed in order to fully break the antiferrimagnetic exchanges: for $\Delta B_0 = 1$ T, $-\Delta S_m$ has a negative -0.7 J kg^{-1} K^{-1} at $T = 0.9$ K. That is, **2** acts as a *cryogenic heater* for this temperature and field range. This inverse behaviour negatively affects the MCE of **2** for large field changes. Complex **1** behaves likewise, although the much weaker antiferromagnetic exchange has a less pronounced effect. In contrast the ferromagnetic exchange observed in complex **3** clearly does favour a very large MCE.

In conclusion, the complexes [Gd$^{III}_4$M$^{II}_8$(OH)$_8$(L)$_8$(O$_2$CR)$_8$](ClO$_4$)$_4$ are molecules in which *almost* all the constituent parts can be exchanged, allowing for a thorough understanding of the individual contributions to the magneto-caloric effect (MCE). In particular, the negative effect of pronounced AF exchange highlights the importance of building ferromagnetic clusters for use in low temperature cooling.

Notes and references

[1] a) M. Evangelisti, F. Luis, L. J. de Jongh, M. Affronte, *J. Mater. Chem.* **2006**, *16*, 2534; b) M. Evangelisti, E. K. Brechin, *Dalton Trans.* **2010**, *39*, 4672.

[2] For recent examples of molecular coolers see: a) M. Evangelisti, O. Roubeau, E. Palacios, A. Camón, T. N. Hooper, E. K. Brechin, J. J. Alonso, *Angew. Chem. Int. Ed.* **2011**, *50*, 6606; b) Y.-Z. Zheng, M. Evangelisti, R. E. P. Winpenny, *Angew. Chem. Int. Ed.* **2011**, *50*, 3692; c) J. W. Sharples, Y.-Z. Zheng, F. Tuna, E. J. L. McInnes, D. Collison, *Chem. Commun.*, **2011**, *47*, 7650; d) S. K. Langley, N. F. Chilton, B. Moubaraki, T. N. Hooper, E. K. Brechin, M. Evangelisti, K. S. Murray, *Chem. Sci.* **2011**, *2*, 1166; J.-B. Peng, Q.-C. Zhang, X.-J. Kong, Y.-P. Ren, L.-S. Long, R.-B. Huang, L.-S. Zheng, Z. Zheng, *Angew. Chem. Int. Ed.* **2011**, *50*, 10649.

[3] See for example: a) A. Benelli, C. Benelli, A. Caneschi, R. Carlin, A. Dei, D. Gatteschi, *J. Am. Chem. Soc.* **1985**, *107*, 8128; b) M. Andruh, I. Ramade, E. Codjovi, O. Guillou, O. Kahn, J. C. Trombe, *J. Am. Chem. Soc.* **1993**, *115*, 1823; c) J. P. Costes, F. Dahan, A. Dupuis, J. P. Laurent, *Inorg. Chem.* **1997**, *36*, 3429; d) A. J. Blake, R. O. Gould, C. M. Grant, P. E. Y. Milne, S. Parsons, R. E. P. Winpenny, *J. Chem. Soc., Dalton Trans.* **1997**, 485; e) C. Benelli, D. Gateschi, *Chem. Rev.* **2002**, *102*, 2369; f) M. Evangelisti, M. L. Khan, J. Bartolomé, L. J. de Jongh, C. Meyers, J. Leandri, Y. Leroyer, C. Mathonière, *Phys. Rev. B: Condens. Matter Mater. Phys.* **2003**, *68*, 184405.

[4] Y.-Z. Zheng, M. Evangelisti, R. E. P. Winpenny, *Chem. Sci.*, **2011**, *2*, 99.

[5] C. Aronica, G. Pilet, G. Chastanet, W. Wernsdorfer, J.-F. Jacquot, D. Luneau, *Angew. Chem. Int. Ed.* **2006**, *45*, 4659.

[6] a) G. Karotsis, M. Evangelisti, S, J. Dalgarno and E. K. Brechin, *Angew. Chem. Int. Ed.* **2009**, *48*, 9928; b) V. Mereacre, M. N. Akhtar, Y. Lan, A. M. Ako, R. Clérac, C. E. Anson, A. K. Powell, *Dalton Trans.* **2010**, *39*, 4918.

[7] S. Piligkos, 2010, Department of chemistry, University of Copenhagen.

[8] A. Bencini, D. Gatteschi, "*Electron Paramagnetic Resonance of Exchange Coupled Systems*", Springer-Verlag, 1990.

[9] W. H. Press, S. A. Teukolsky, W. T. Vetterling, B. P. Flannery, *"Numerical Recipes in C: The Art of Scientific Computing"*. Second Edition, Cambridge, Cambridge University Press, 1992.

[10] (a) J. Jaklič, P. Prelovsěk, *Phys. Rev. B*, **1994**, *49*, 5065; (b) J. Schnack, O. Wendland, *Eur. Phys. J. B*, **2010**, *78*, 535.

[11] J. Schnack, P. Hage, H.-J. Schmidt, *J. Comput. Phys.* **2008**, *227*, 4512.

[12] A.J. Blake, C.M. Grant, S. Parsons, J.M. Rawson, R.E.P. Winpenny, *J. Chem. Soc., Chem. Commun.*, **1994**, 2363-2364.